

**Supplemental Table 1. Intermolecular interactions in TGF- $\beta$ 1/T $\beta$ RI/T $\beta$ RII ternary complex**

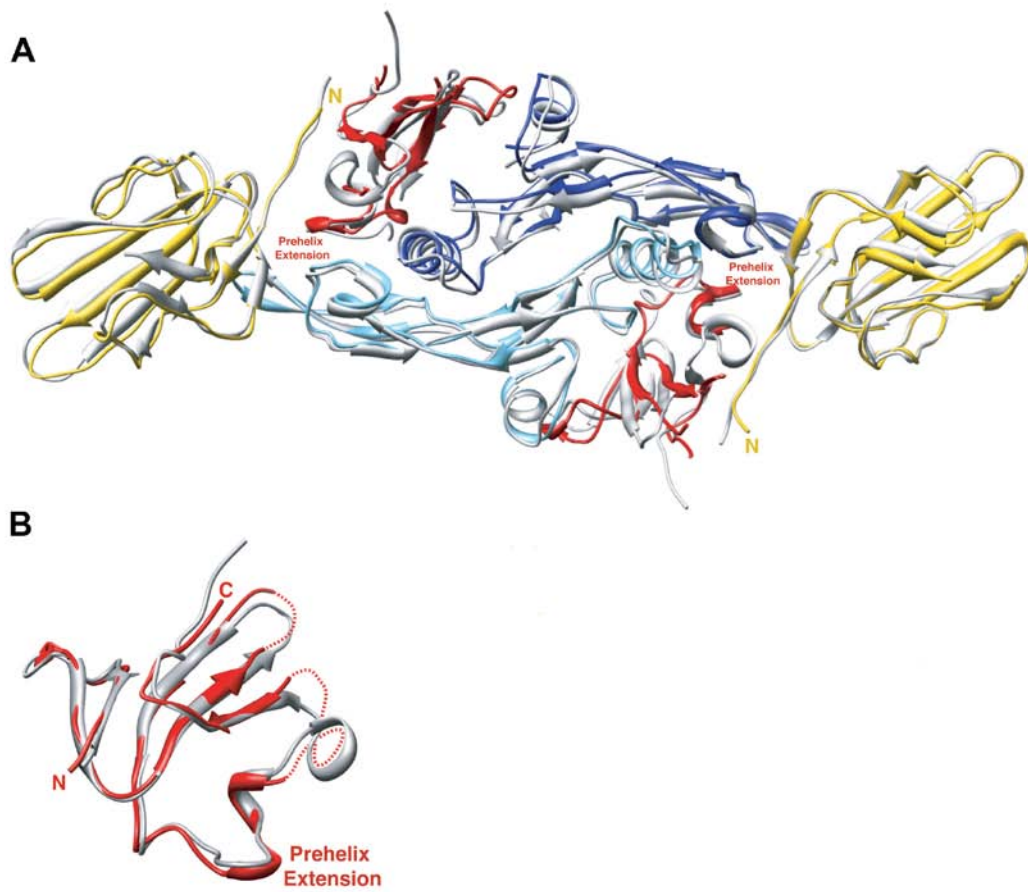
Residue/Atom	Residue/Atom	Distance (Å)
<b>TGF-<math>\beta</math>1</b>	<b>T<math>\beta</math>RII</b>	
<i>Hydrogen bonds and salt bridges</i>		
Arg 25 Nh1	Glu 119 O $\epsilon$ 1	3.5
Arg 25 Nh2	Glu 119 O $\epsilon$ 2	2.6
His 34 N $\epsilon$ 2	Ser 49 O	2.8
Tyr 91 O	Ile 53 N	2.8
Gly 93 N	Ile 53 O	2.9
Gly 93 O	Ser 52 O $\gamma$	3.2
Arg 94 Nh1	Asp 32 O $\delta$ 1	2.6
Arg 94 N $\epsilon$	Asp 32 O $\delta$ 2	2.9
<i>Hydrophobic contacts</i> <sup>a</sup>		
Tyr 91	Ile 50, Ser 52	
Arg 94, Gly 93	Phe 30	
<b>TGF-<math>\beta</math>1 (A)</b>	<b>T<math>\beta</math>RI</b>	
<i>Hydrophobic contacts</i>		
Trp 30	Phe 60	
Trp 32, Tyr 90	Pro 55	
Leu 101	Ile 54	
<b>TGF-<math>\beta</math>1 (B)</b>	<b>T<math>\beta</math>RI</b>	
<i>Hydrogen bonds</i>		
Tyr 6 OH	His 15 N $\epsilon$ 2	3.2
<i>Hydrophobic contacts</i>		
Ala 1, Leu 2, Tyr 6	Leu 16	
Asn 5	Lys 19	
Tyr 6	His 15, Leu 16	
Ile 51	Phe 31	
Gln 57	Ile 54	
Lys 60	Val 61	
<b>T<math>\beta</math>RII</b>	<b>T<math>\beta</math>RI</b>	
<i>Hydrophobic contacts</i>		
Ala 21	Cys 77	
Val 22	Leu 29, Cys 76, Cys 77, Asn 78	
Phe 24	Leu 29, Pro 59	
Pro 25	Arg 58	
Leu 27	Arg 58	
Ile 53	Arg 58	

<sup>a</sup> Carbon-carbon contacts  $\leq 4.0$  Å

## FIGURE LEGENDS

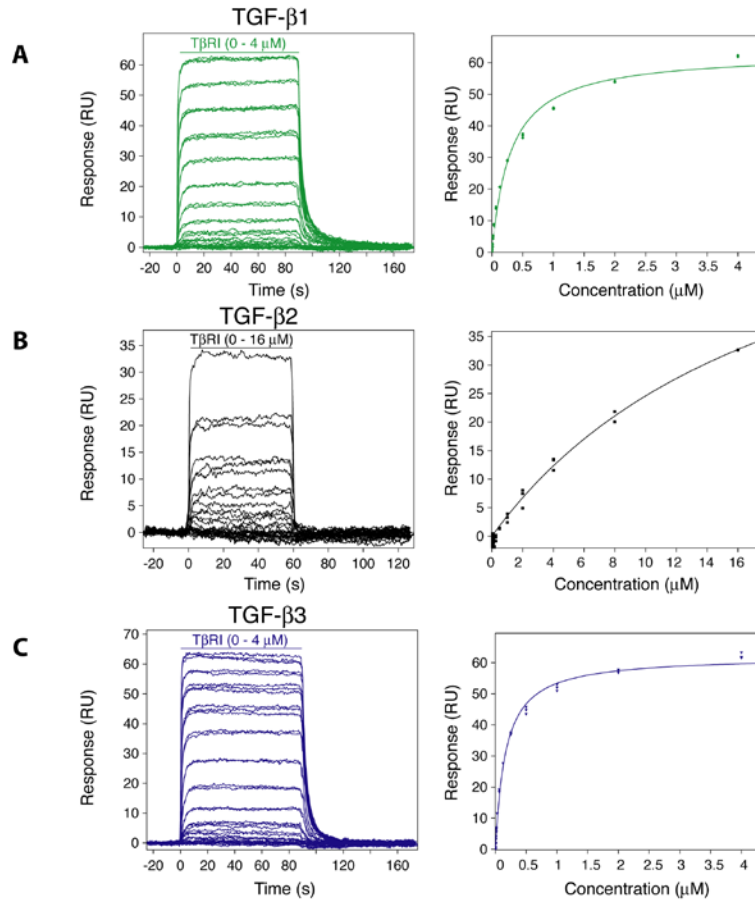
**Supplemental figure 1.** Structural superposition demonstrating overall similar manner of complex assembly observed with TGF- $\beta$ 1 and - $\beta$ 3. (A) Overlay of TGF- $\beta$ 1 and - $\beta$ 3 ternary complex structures. Structures were superimposed using the full ligand dimer and the corresponding bound T $\beta$ RII. Components of the TGF- $\beta$ 1 ternary complex are colored (TGF- $\beta$ 1<sub>A</sub>-monomer – light blue, TGF- $\beta$ 1<sub>B</sub>-monomer – dark blue, T $\beta$ RI – red, T $\beta$ RII – yellow) whereas those of the TGF- $\beta$ 3 ternary complex are grey. (B) Overlay of T $\beta$ RI from the TGF- $\beta$ 1 and TGF- $\beta$ 3 ternary complexes (red and grey, respectively) showing that the structures are overall very similar (in spite of its somewhat different positioning in the two ternary complexes; Fig 1C).

**Supplemental figure 2.** SPR equilibrium analysis of the interaction between T $\beta$ RII and TGF- $\beta$ 1, TGF- $\beta$ 2 and TGF- $\beta$ 3 and between T $\beta$ RI and TGF- $\beta$ 2 and TGF- $\beta$ 3. (A-C) Sensorgrams and binding isotherms obtained as T $\beta$ RII was injected. Traces correspond to triplicate measurements of 2-fold serial dilutions of the receptor over the ranges shown. Surface densities were 185, 339, and 165 resonance units (RU) for TGF- $\beta$ 1 (A), - $\beta$ 2 (B), and - $\beta$ 3 (C), respectively. Binding isotherms correspond to plots of the response at equilibrium as a function of receptor concentration, which were fit to a hyperbolic equation using Scrubber 2 software. (D-E) Sensorgrams and binding isotherms obtained as T $\beta$ RI was injected. Traces correspond to triplicate measurements of 2-fold serial dilutions of the receptor over the ranges shown. Surface densities were 339 and 451 resonance units (RU) for TGF- $\beta$ 2 (D), and - $\beta$ 3 (E), respectively. Data is not shown for TGF- $\beta$ 1 since the maximum binding observed (8 RU at 16  $\mu$ M on a 686RU surface) was too weak to permit an equilibrium analysis.



Supplemental Figure 1

## T $\beta$ RII Binding



## T $\beta$ RI Binding

